CHAPTER

26 Radio and radar astronomy

Radio astronomy was discovered accidentally in 1931 by Karl Jansky, a physicist at Bell Telephone Laboratories. Jansky had been assigned to identify the sources of noise encountered in a newly installed transatlantic short-wave radiotelephone service. Using a directional receiving antenna on 20.5 MHz, he observed that one component of the noise, a wideband hiss, had a diurnal variation that reached a maximum intensity on average four minutes earlier each day. Jansky knew that the stars advance in just this way (in siderial time) and deduced that the source of the hiss must be outside the solar system. His observations showed that this "cosmic noise" came from the galactic plane and was strongest from the direction of the galactic center (in the constellation Sagittarius).

After Jansky, the second pioneer of radio astronomy was a radio engineer, Grote Reber, who in 1937, built a 9-m (30-ft) parabolic reflector beside his house in Wheaton, Illinois. This was maybe the first modern dish antenna. Reber began his observations using a receiver at 3 GHz, which pushed the high-frequency state of the art, because he assumed that cosmic radio noise was the low-frequency tail of the thermally generated radiation spectrum from white-hot stars. The intensity of this radiation would increase as the square of the frequency, so using the highest practical frequency would make detection easier and would also make his antenna more directive. Detecting nothing at 3 GHz, he worked his way down finally to 160 MHz, where he was able to make contour maps of the cosmic noise intensity. The radiation he and Jansky observed is now known to be *synchrotron radiation*, caused by the centripetal acceleration of fast, i.e., non-thermal, electrons spiraling in a magnetic field. By the end of World War II, the Sun (an ordinary thermal source under low sunspot conditions) had been detected at microwave frequencies. After the war, a previously-predicted spectral line at 21 cm (1420 MHz) was quickly detected. This famous neutral hydrogen line corresponds to the energy difference between the parallel and antiparallel orientations of the magnetic moment of the nucleus (the proton) with respect to the magnetic moment of the spinning electron. Many radio telescopes have been built in the decades following the war, the largest being the

305-m (1000-ft) diameter dish built by Cornell University at Arecibo, Puerto Rico. Discoveries in radio astronomy include some one hundred atomic recombination and molecular lines, pulsars, natural masers, and the isotropic 3K blackbody cosmic background radiation, a remnant left from the Big Bang.

26.1 Radiometry

Most of the radio sources found in nature emit wideband noise; their radiation comes from a great number of individual radiators whose contributions add randomly to produce *Gaussian noise*. (A histogram of voltage samples from the antenna terminals forms a Gaussian curve centered on zero.) Since such a signal is itself a random process, we can only measure its average properties. The most important of these is the average of the square of the voltage, i.e., the power. If we take, say, several n-minute averages of the power, these averages will be scattered around the true average. If n is made larger, the averages will be distributed more tightly about the true average. It might not take long to measure the receiver output power to a precision of, say, 10% or even 1%. But that is almost never long enough to measure the power of a radio source to the same precision or, for that matter, even to detect a source. The problem is that the power from the source is masked by other sources of noise including receiver noise, antenna noise, and cosmic background noise. When an astronomer is trying to detect a source in a certain direction, the first step is to average the power received from that direction, the on-source direction. The next step is to measure the power from a nearby, but off-source, direction. Finally, the latter "off" power is subtracted from the former "on" power. For weak sources (most sources), these powers are almost identical and might correspond to a system temperature[1] of, say, 100 K. Yet the astronomer may need to detect a source that raises the system temperature by only 10 mK. This requires that the "on" and the "off" powers both be measured to an accuracy of, say, $3.3/\sqrt{2} = 2.3$ mK for a 3-sigma detection. The fractional accuracy of the "on" and "off" power measurements must therefore be $0.0023/100 = 2.3 \cdot 10^{-5}$ or about one part in 50 000 (see Problem 26.1).

If we average N samples of the squared voltage, the relative standard deviation, $\delta P/P$, will be $\sqrt{2/N}$ if the voltage has a Gaussian distribution and if all the samples are independent (see Problem 26.2). A signal from a channel of bandwidth, B, can furnish $2B$ independent samples every second. Integrating for a time T we can therefore collect $2BT$ independent samples and the relative standard deviation of the power measurement will therefore be

[1] A *system temperature* of 100 K, for example, means that the equivalent noise power at the receiver input is the same as the noise power from a resistor at 100 K. This equivalent noise power is the sum of the actual noise power (sky noise from the main lobe, ground noise picked up from back-lobes, some thermal noise if the antenna is lossy, plus a contribution representing the noise generated in the receiver.

$$\delta P/P = (BT)^{-1/2}. \tag{26.1}$$

Usually a radio astronomer expresses power in terms of antenna temperature and would write $\delta T/T_{\text{system}}$ rather than $\delta P/P$. Equation (26.1) is commonly known as the "radiometer equation." Note that sensitivity increases with bandwidth, contrary to many communication situations where increasing the bandwidth just increases the noise and decreases the signal-to-noise ratio. We arrived at Equation (26.1) by considering digital (discrete) signal processing. It is also common to use an analog square-law detector followed by an analog lowpass filter, which does the averaging. When the lowpass filter is just a simple *RC* integrator, an analog signal analysis shows that the radiometer equation can be written as

$$\delta T/T_{\text{sys}} = (2BRC)^{-1/2}. \tag{26.2}$$

26.2 Spectrometry

Many sources produce "colored" noise rather than white noise, i.e., the flux density from these sources varies with frequency. Often these variations reveal characteristic shapes of atomic or molecular lines. Instead of just measuring the total power, the signal is divided into adjacent frequency "bins" and the power in each bin is measured. When a spectrum of bandwidth B is divided into n frequency bins, each of bandwidth B/n, the radiometer equation shows that the integration time must be increased by n. It is therefore especially important in radio astronomy, where weak sources may require many hours of integration, to measure the n individual spectra simultaneously rather than sequentially. Simultaneous analysis is done with multichannel radiometers ("multiplex" spectrum analyzers). The simplest multiplex spectrometer is just a bank of n filters, each followed by its own square-law detector and averager. Such an instrument is called a filterbank, but might better be called a radiometer bank. Today, most radio spectrometry is done digitally, often using digital *autocorrelators* (see Chapter 27).

26.3 Interferometry

The classic single-dish radio telescope such as Reber's backyard dish or the Arecibo dish has an angular resolution which is diffraction limited; the angular size of the beam (between half-power points) is about λ/D radians where D is the diameter of the dish. Such a telescope can make maps by scanning the vicinity of a source and doing radiometric averages at each point, but the resolution of the map is limited to λ/D. Better resolution requires a larger antenna. Interferometry uses more than one antenna to form a beam whose size

corresponds to the *spacing* between the antennas rather than their diameters. The simplest interferometer has just two elements. The beam formed by the two antennas together has a series of narrow lobes in one dimension. If a point source moves across these lobes, the radiometer will trace out the lobes, just as a point source moving across the beam of a single dish antenna traces out the beam pattern. (Of course the interferometer's fine lobe structure is multiplied by the broader beam pattern of the individual antennas.) The multilobed pattern of a two-element interferometer is unsuitable for the intensity mapping described above but it is often used to set an upper limit on the angular size of a source.

26.3.1 Imaging interferometry

By using data from multiple antennas, it is possible to synthesize a beam that is small in both dimensions, i.e., a beam that would correspond to a filled-aperture antenna whose diameter is the size of the interferometer array. The VLA (Very Large Array) at Socorro, New Mexico, is an example of such a system. Signals from 27 antennas are transmitted up to 21 km through optical fibers (originally through low-loss circular waveguides) to the central processing laboratory. The VLBA (Very Long Baseline Array) has 10 antennas with spacings as large as the distance from Hawaii to St. Croix in the Virgin Islands. Its signals, together with timing information, are recorded on magnetic media at each station and sent, physically or electronically, to New Mexico for after-the-fact combining and processing. Imaging interferometers (phased arrays) work essentially as follows. Suppose we have an array of antennas such as shown in Figure 26.1. Assume the antennas are all pointed in the same direction,

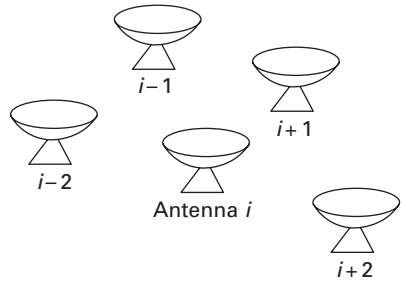

Figure 26.1. An interferometer antenna array.

say up. If the voltages from the antennas are all added together in phase, squared, and averaged, the result is a narrow beam, pointing straight up. This process can be written as follows:

$$P_0 = \left\langle \sum_n V_n^2 \right\rangle = \sum_{n,m} \langle V_n V_m^* \rangle. \tag{26.3}$$

Now suppose we add the voltages, multiplied by a progressive phase shift, to form a beam tilted slightly off the vertical. If we do this addition, followed by squaring and averaging, we get the k-th beam:

$$P_k = \left\langle \sum_{n,m} V_n e^{j\phi_{n,k}} V^* e^{-j\phi_{m,k}} \right\rangle = \sum_{n,m} e^{i(\phi_{n,k}-\phi_{m,k})} \langle V_n V_m^* \rangle. \quad (26.4)$$

This is the general case; for the straight-up beam, $\phi_{n,k}$ and $\phi_{m,k}$ are both zero. The important thing to notice is that we can multiply the signals from every possible antenna pair and average the products first, independent of what beam we wish to form. After averaging these pairs we can *then* form each beam by weighting the averaged products with the appropriate phase factors and performing the double sums. Note also that the averaged products do not have to be measured simultaneously; we could even use one fixed antenna and one mobile antenna and measure the average product for one baseline after another. The VLA has 27 antennas so it can measure $(27 \times 26)/2$ baselines simultaneously. But, as the Earth turns, these baselines become different baselines so, over time, it is possible to collect averaged products from a huge number of baselines. This set of baselines is virtually the same as all the baselines one could form between pairs of points on a dish with a radius of 21 km, and the final synthesized beam can be as sharp and clean as if it had come from a filled dish. An array can thus have the resolution of an enormous antenna even if it does not have the corresponding sensitivity (collecting area). On the other hand, because the individual antenna elements have relatively wide beams, an array has a relatively wide field of view. Radio astronomers hope to have, by the year 2020, a super large array, the SKA (see reference 5) which would have a total collecting area of one square kilometer and provide baselines as long as 3000 km.

26.4 Radar astronomy

Ionized meteor trails produced echoes on WWII radars, but echoes from the Moon were not observed until after the war. In January 1946, a U.S. Army Signal Corps group headed by John H. DeWitt, Jr. observed real-time Moon echos using modified WWII radar equipment delivering 3 kW of power at 110 MHz to a 64-element dipole antenna array. In Hungary, one month later, Zoltán Bay used similar equipment, together with electrolytic cells ("coulombmeters") to do signal integration. By the end of his experiment, the on-target cell had accumulated significantly more gas than the off-target cell. Many large radars were built in the late 1950s, and radar echo detections from the Sun, Venus, Mercury and Mars were made in the 1960s. Radar was used to measure the rotation rates of Venus and Mercury. Saturn's rings were detected in the 1970s, as were the large moons of Jupiter, many asteroids and several comets.

26.4.1 The Moon

The Moon's distance from the Earth, R, is 3.8×10^5 km, and it has a *radar cross-section,* σ, of about 6.6×10^5 km^2. This means that the power density of the

echo's *S*R, in watts per square meter, received back on the radar antenna will be given by $\sigma/(4\pi R^2)$ times the power density incident on the target, S_{inc}. (Note that this defines *radar cross-section* as the collecting area of an equivalent target that isotropically scatters the intercepted incident power.) The incident power density is just $S_{inc} = P_T G/(4\pi R^2)$, where P_T is the transmitter power and G is the antenna gain. The power into the receiver, P_R, is equal to $S_R A_{eff}$ where A_{eff} is the effective collecting area of the antenna. We have seen earlier that G is equal to $4\pi A_{eff}/\lambda^2$. The Moon's radar cross-section is about 7% of its geometric cross-section, i.e., it is 7% as reflective as a metal sphere of the same size. An echo from the Moon will therefore produce a power at the receiver of

$$P_R = P_T \frac{4(\pi A_{eff}/\lambda^2)}{4\pi R^2} \frac{\sigma}{4\pi R^2} A_{eff} = \frac{P_T A_{eff}^2 \sigma}{4\pi R^4 \lambda^2}. \quad (26.5)$$

Suppose we have a radar with a 1-kW transmitter and a modest 5-m diameter dish antenna with an aperture efficiency of 50%. The effective area of this antenna is therefore half of its geometric cross-section or $A_{eff} = 0.5 \times \pi (5/2)^2 = 9.8\,m^2$. It is an experimental fact that σ for a planet is approximately independent of wavelength, so we see from Equation (26.5) that the received power is inversely proportional to λ^2 (because of the fundamental antenna relation between gain and effective area). Suppose that the wavelength is 30 cm, i.e., the frequency is 1 GHz. With this radar system, the power received from the Moon would be

$$P_R = \frac{1000\,W(9.8\,m^2)^2 6.6 \times 10^{11}\,m^2}{4\pi(3.8 \times 10^8\,m)^4 (0.30\,m)^2} = 2.7 \times 10^{-18}\,W. \quad (26.6)$$

Whether this amount of power is easy to detect or not depends on the noise it competes with. Let us assume that the noise from the antenna (sky noise from background cosmic radio sources plus some "spill-over" noise from the surrounding ground) has an equivalent noise temperature, $T_{ant} = 50$ K. Let us also assume that our receiver has an equivalent noise temperature, $T_{rcvr} = 35$ K. The total equivalent input temperature is therefore given by $T_{system} = 85$ K and the noise power will be $kT_{sys}B$. If we make the bandwidth, B, very small we decrease the noise power and hence detection becomes easier. But if we make B very small we will need a very accurate prediction of the Doppler shift caused by the relative motion of the Earth and Moon in order to tune the return echo into the passband of the filter. Finally, the rotation of the Moon causes a Doppler *broadening* of the return echo; if we make B less than 25 Hz we will begin to exclude some of the broadened signal. Let us compromise and use a bandwidth of 100 Hz. The signal-to-noise ratio at the receiver output will then be given by

$$S/N = \frac{P_R}{kT_{sys}B} = \frac{2.7 \times 10^{-18} W}{1.38 \times 10^{-23}\,W/Hz/K \times 85\,K \times 100\,Hz} = 23.0. \quad (26.7)$$

This SNR of 23 is large enough that the signal would be visible on an oscilloscope connected at the intermediate frequency (IF) voltage output; no signal averaging would be needed. The modest radar system assumed here could be assembled for a few thousand U.S. dollars.

26.4.2 Venus

Venus is not nearly so easy to detect, being some 280 times more distant than the Moon. Its radar cross-section is about 20 times that of the Moon, so with the radar system described above, the SNR of the return echo would be lower by a factor $280^4/20$ or 307 million! This requires a *much* larger radar. The Arecibo radar, however, has an effective antenna diameter of 200 meters and an average power of 1 MW at 2.38 GHz. It would out-perform our Moon example radar by a factor of $(10^6/10^3)\ (2.38/1)^2\ (200^2/5^2)^2$ or 1.4×10^{10}. Thus, with the same assumed bandwidth and system temperature, the Venus echo from the Arecibo radar would have an SNR of 23 $(1.4 \times 10^{10})/(307 \times 10^6) = 1090$. This is overkill for a simple detection but is needed for high-resolution mapping.

26.4.3 Delay-Doppler mapping

Except for the Moon, planetary targets have angular sizes much smaller than the radar beam. Nevertheless, images of photographic quality can be made by a technique known as delay-Doppler mapping. This method uses short pulses (or pulse compression) to obtain adequate range resolution. The relative motion between the radar and the target provides resolution in the transverse direction via the Doppler effect. This was the method used to get the first surface images of Venus, whose cloud cover kept its features hidden to optical telescopes. The technique is essentially the same as side-looking or synthetic aperture radar by which photographic-like images of ground targets are made from an airborne radar with only a small dish antenna. Figure 26.2 shows how delay-Doppler mapping works. This is a view of the planet as seen from the radar. When a short pulse is transmitted, the first echo to return comes from the front cap or sub-Earth point. At subsequent times the echo signal

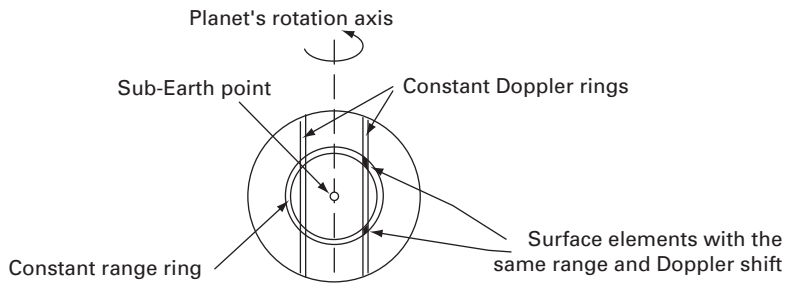

Figure 26.2. Geometry for delay-Doppler radar imaging.

corresponds to loci of equal range that are rings on the planetary surface, centered on the sub-Earth point. Because the planet is rotating, surface points on the right-hand side are moving away from the radar and their echoes are Doppler-shifted to lower frequencies. Likewise, points on the left-hand side are up-shifted. The magnitude of the of Doppler shift is proportional to the cross-range distance, i.e., the distance in the direction perpendicular to both the planet's axis of rotation and the line between the radar and the planet. Loci of constant Doppler shift are rings parallel to the rotation axis of the planet and to the line from the planet to the radar.

The two shaded surface elements have the same range and the same Doppler shift. This fundamental ambiguity can be removed, at least for Venus maps made at Arecibo, by tilting the radar beam slightly to illuminate only the Northern or only the Southern hemisphere of Venus. Obviously this technique requires the narrow beam provided by a very large antenna. Data taking is done as follows: a series of IF voltage samples is read and stored separately as each return pulse arrives. After many pulses have been received, we have a time series for each range ring. Each series is Fourier analyzed to get the Doppler spectrum. The magnitude of a given Doppler component corresponds to the reflectivity of the surface element at the intersection of the range ring and the Doppler ring.

26.4.3.1 Overspreading

The standard delay-Doppler[2] method will not work when the planet is too large and/or spins too fast. This is because the Nyquist sampling theorem requires that the (complex) sampling rate be at least equal to the bandwidth of the signal so that high-frequency Doppler components do not "alias" and appear as lower frequency components (the stroboscope effect). This establishes a minimum pulse repetition frequency (PRF). But if the depth of the planet is too large, even the minimum PRF will result in having more than one pulse on the planet at a time, causing the echoes from different ranges to "fold" together.

The bandwidth of the return echo (twice the highest Doppler shift) is given by $B = 2f_{\text{radar}}\, 2v_{\max}/\text{c} = 4f_{\text{rad}}r_{\text{planer}}\, \Omega\, /c$ where r_{planet} is the radius of the planet, Ω is its apparent angular velocity,[3] f_{radar} is the frequency of the radar, and α is the angle between the radar beam from the Earth and the planet's rotation axis. Therefore, the Nyquist sampling requirement is $f_{\text{sample}} > 4f_{\text{radar}}\, r_{\text{planet}}\, \Omega/c$. The condition to avoid range folding is $1/f_{\text{sample}} > 2\text{r}_{\text{planet}}/\text{c}$. Multiplying these two inequalities gives us $1 \geq 8\, f_{\text{radar}}\, r^2_{\text{planet}}\, \Omega/\text{c}^2$, which imposes an upper limit on the frequency of the radar:

[2] Note that delay-Doppler mapping of space objects is the same technique as pulse-Doppler radar, discussed in Chapter 21. But while the planet presents a "target" in every range-Doppler cell, a pulse-Doppler surveillance radar is likely to have a target (often an airplane) in only a single range-Doppler cell.

[3] The *apparent* angular velocity of the planet corrects for the planet's tilt and the relative translational (orbital) motion of the Earth and the planet.

$$f_{\text{radar}} < \frac{c^2}{8r^2\Omega}. \tag{26.8}$$

Using Equation (26.8), the radar frequency should be less than about 1.5 GHz for Venus and less than about 1.8 GHz for Mercury. These are practical frequencies for conventional microwave radar technology. For Mars, however, the radar frequency would have to be lower than 14 MHz, because of the high rotation rate. Equation (26.5) shows that such a low frequency would require an extremely large antenna. To make matters worse, sky noise and atmospheric noise at 14 Mz are both much higher than at microwave frequencies.

While standard delay-Doppler does not work for Mars and other overspread targets, Mars images were made in 1988 using the VLA in New Mexico. During the observations, Mars was illuminated with a 10-GHz signal from the JPL NASA Solar System Radar transmitter at Goldstone, California. The resolution of these images was only about 100 km.

A modified delay-Doppler technique, developed around 1986 for radar probing of the ionosphere, was first used at Arecibo in 1990 to solve the overspreading problem for Mars. This "long code" technique is used with the 2.38-GHz transmitter, which puts out a continuous wave (cw) rather than pulsed power, but is biphase-modulated with a long pseudorandom code – for Mars, a sequence of 10-μs bauds. The code elements shift the RF phase by zero or 180°, equivalent to leaving the signal unchanged or changing its polarity. The length of the sequence must be greater than 0.33 seconds (the length of a coherent integration or "look"), though the sequence used at Arecibo repeats only every 3054 hours and can be considered totally random. To see how this technique works, imagine first a simple point target. The echo from such an object would be a delayed version of the code. At the receiver we sample the return echo at the baud rate and multiply successive samples of the echo signal by successive bauds of an identical "replica" code to undo the echo's phase reversals. When the replica code has the correct alignment, it undoes the phase reversals and produces a cw signal. We can separately multiply the echo samples by the replica code for all alignments. Identifying the alignment that produces a cw signal gives us the distance (range) to the point target. If the point target has a velocity component parallel to the radar beam, the recovered cw signal will be Doppler shifted and we can determine the velocity component. Next, imagine that the echo comes from *two* point reflectors, separated in time by at least one baud (1500 m in range). Again multiplying the echo by the replica code, we would find two alignments that produce cw signals and could thereby deduce the range and line-of-sight velocity of each target. Note, however, that the "decoded" signal from either target contains white noise that is the signal from the other target, randomized because the replica code is not aligned with its echo. This "self-noise" has power equal to that of the desired signal, assuming the targets have equal radar cross-sections. We can consider the range rings on a planet to be a set of N such targets, separated in range delay by the

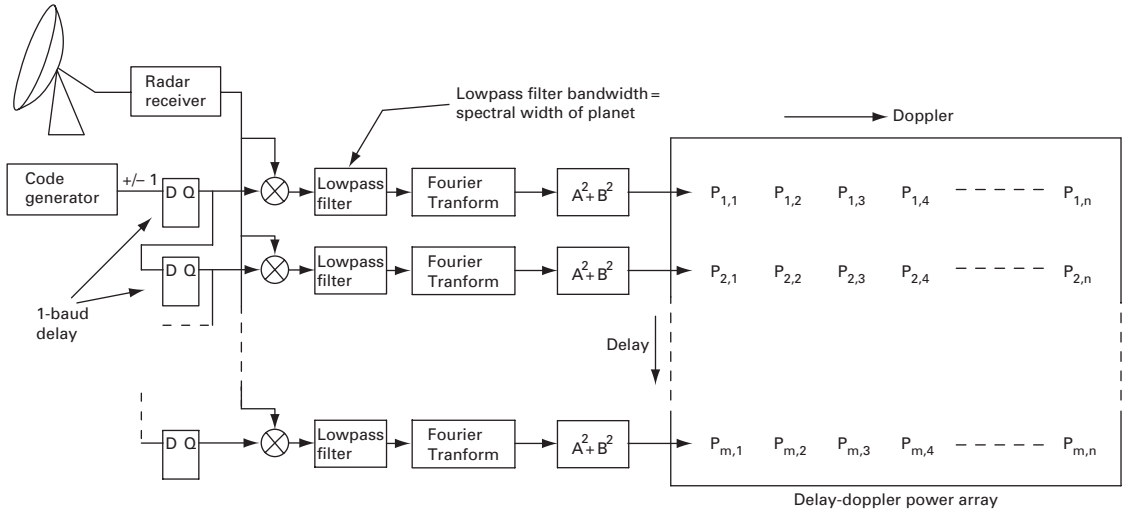

Figure 26.3. Long-code delay-Doppler method.

baud length. (Each range ring has a Doppler spectrum.) The self-noise voltage is therefore the sum of N voltages, which add as a random walk. The delay time depth of Mars is 23 ms so, for a baud length of 10 μs, $N = 2300$. If we assume that the signals from the rings are approximately equal in strength, the self-noise power will be N times the signal power. Here, this factor can be reduced to 2300 $(7.5/100) = 177$ by lowpass filtering the data sequences before doing the Doppler analysis, since the self-noise is spread out over a much larger bandwidth (100 kHz) than the Mars echo bandwidth (7.5 kHz). This still appears disastrous, until we remember that the self-noise is in addition to "real" noise, i.e., cosmic noise, antenna noise, and receiver noise. Under the worst weak-signal conditions, the self-noise is insignificant compared to the real noise so, while the system performance will be poor, the self-noise is not to blame. Under the best conditions, the self-noise dominates the real noise and it will determine the integration time needed to pull the signal out of the total noise. When the long-code technique is used with the Arecibo S-band radar system to observe Mars, the effective signal-to-noise ratio is decreased by a factor of 5.2 or 1.7, depending on the polarization of the echo.[4] Figure 26.3 shows a signal processing arrangement that produces the decoded signals for each range, does a Fourier transform on each decoded range signal, and stores the resulting delay-Doppler data points in an array.

[4] The radar transmits a signal with circular polarization. Smooth portions of the planetary surface create specular (mirror-like) reflections, which reverse the sense of the circular polarization. Rough portions of the surface create multipath reflections, which cause some of the echo power (usually less than half) to return with the same circular sense as the transmitted signal. The radar is equipped to receive both polarizations.

Problems

Problem 26.1. Use the radiometer equation to find how much time is needed to make a 3-sigma detection of a 10 mK radio source if the radio telescope's system temperature is 100 K. Assume the predetection bandwidth, B, is 10 MHz. A "3-sigma detection" requires that the 0.01 K contribution from the source be $3\sqrt{2}$ times the δT fluctuation predicted by the radiometer equation. (The factor $\sqrt{2}$ takes account of the increased fluctuation when the "off" is subtracted from the "on", assuming an equal time T is spent measuring each.)

Problem 26.2. Verify that if a noise power estimator is defined as the average of N independent samples of the squared noise voltage, the standard deviation of this estimator will be $\sigma^2\sqrt{2/N}$. Assume that the probability distribution of the noise voltage is Gaussian with zero mean and variance σ^2. Hint: for a zero-mean Gaussian distribution, the expected value of V^2 is σ^2 and the expected value of V^4 is $3\sigma^4$.

Problem 26.3. Pulsars (rotating neutron stars) are radio sources that turn on and off with very regular periods ranging from about 2 milliseconds to about 2 seconds. Given a radio telescope at your disposal, how would you go about searching for pulsars, i.e., what kind of data processing scheme would you use to find these periodic sources?

References

[1] Butrica, A. J., *To See the Unseen: A History of Planetary Radar Astronomy*, Diane Publishing Co., 1997 (also available on the Web).
[2] Goldsmith, P. ed. *Instrumentation and Techniques for Radio Astronomy*, IEEE Press,1988. (This book is prefaced with 12-page historical overview.)
[3] Kraus, J. D., *Radio Astronomy*, 2nd edn, Cygnus-Quasar Books, 1986.
[4] Ostro, S. J., Planetary radar astronomy, *Rev Mod Phys*, Vol. **65**, No. 4, pp. 1235–1279, October 1993.
[5] http://www.skatelescope.org/PDF/SKABrochure_2007.pdf